

# CEBAF Program Advisory Committee Nine Proposal Cover Sheet

This proposal must be received by close of business on Thursday, December 1, 1994 at:

CEBAF  
User Liaison Office, Mail Stop 12 B  
12000 Jefferson Avenue  
Newport News, VA 23606

## Proposal Title

A Detailed Study of Nuclear Structure Functions  $F_2(x_b)$  and  $R(x_b)$   
in the Valence Quark Region.

## Contact Person

Name: A. Saha  
Institution: CEBAF  
MS 12H, Physics Division  
Address: 12000 Jefferson Avenue  
Address: Newport News, VA 23606, USA  
City, State ZIP/Country:  
Phone: (804) 249-7606 FAX: (804) 249-7363  
E-Mail → Internet: SAHA@CEBAF.GOV

Experimental Hall: A Days Requested for Approval: 19

Hall B proposals only, list any experiments and days for concurrent running:

## CEBAF Use Only

Receipt Date: 12/13/94 PR 94-105

By: gs

# PROPOSAL TO THE CEBAF PAC9

## A Detailed Study of Nuclear Structure Functions $F_2(x_b)$ and $R(x_b)$ in the Valence Quark Region.

### Spokespersons

N. Bianchi

*INFN-Laboratori Nazionali di Frascati, ITALY*

J. Gomez, A. Saha (Contact Person)

*Continuous Electron Beam Accelerator Facility, Newport News, VA*

### Hall A Collaboration Proposal

#### List of Institutions

*INFN-Laboratori Nazionali di Frascati, ITALY*

*CEBAF, Newport News, VA*

*College of William and Mary, Williamsburg, VA*

*University of Virginia, Charlottesville, VA*

*University of Maryland, College Park, MD*

*Massachusetts Institute of Technology, Cambridge, MA*

*Rutgers University, Piscataway, NJ*

*Kent State University, Kent, OH*

*Cal. State University, Los Angeles, CA*

*Old Dominion University, Norfolk, VA*

*Kharkov Institute of Physics and Technology, Kharkov, UKRAINE*

*Yerevan Physics Institute, Yerevan, ARMENIA*

*University of Georgia, Atlanta, GA*

*Chungnam National University, Taejon, KOREA*

*University of Kentucky, Lexington, KY*

*Submitted: December 13, 1994*

### Abstract

We propose an inclusive electron scattering measurement on different nuclei to investigate the bound nucleon structure functions in the valence quark region ( $0.1 < x_b < 0.6$ ). Precise data would allow one to measure for the first time nuclear medium effects in both structure functions  $F_2(x_b)$  and  $R(x_b) = \sigma_L(x_b)/\sigma_T(x_b)$  and to disentangle between nucleonic and non nucleonic effects in few-nucleon systems, where microscopic calculations are more reliable.

## List of Participants

- N. Bianchi (Spokesperson), G.P. Capitani, E. De Sanctis, P. Levi Sandri,  
V. Muccifora, E. Polli, A.R. Reolon, P. Rossi  
*INFN-Laboratori Nazionali di Frascati, ITALY*
- J.P. Chen, J. Gomez (Spokesperson), J. LeRose, R. Michaels, S. Nanda  
A. Saha (Contactperson), B. Wojtsckhowski  
*Continuous Electron Beam Accelerator Facility, Newport News, VA*
- K.A. Griffioen, J.M. Finn, J. McIntyre  
*College of William and Mary, Williamsburg, VA*
- H. Baghaei, D. Crabb, D. Day, J. McCarthy, R. Lindgren, R. Lourie, O. Rondon-Aramayo  
*University of Virginia, Charlottesville, VA*
- C.C. Chang, P. Markowitz  
*University of Maryland, College Park, MD*
- W. Bertozzi, S. Gilad, A. Sarty  
*Massachusetts Institute of Technology, Cambridge, MA*
- R. Gilman, C. Glashauser, R. Ransome, E. Brash, L. Bimbot  
*Rutgers University, Piscataway, NJ*
- B.A. Anderson, D. Madey, D.M. Manley, G. Petratos, J.W. Watson, W.-M. Zhang  
*Kent State University, Kent, OH*
- K. Aniol, M. Epstein, D. Margaziotis  
*Cal. State University, Los Angeles, CA*
- P. Ulmer  
*Old Dominion University, Norfolk, VA*
- A. Afanasev, A. Glamazdin, V. Gorbenko, L. Levchuk, P. Sorokin  
*Kharkov Institute of Physics and Technology, Kharkov, UKRAINE*
- A. Gasparian, A. Voskanian  
*Yerevan Physics Institute, Yerevan, ARMENIA*
- P. Rutt, F.T. Baker  
*University of Georgia, Atlanta, GA*
- D. Dale  
*University of Kentucky, Lexington, KY*
- J.C. Yang  
*Chungnam National University, Taejon, KOREA*

## INTRODUCTION

The so called “EMC effect” discovered during the 1980’s<sup>[1]</sup>, has caused a big controversy in the community of nuclear and high energy physicists. During the last ten years, experiments have been performed in three different laboratories and hundreds of papers about the possible interpretation of the modification of the nucleon structure functions inside nuclei have been published. However, from the experimental point of view, the main goal of four experiments (EMC<sup>[1]</sup>, BCDMS<sup>[2]</sup>, NMC<sup>[3]</sup>, FNAL E665<sup>[4]</sup>) has been to emphasize the region of low  $x_b$  (see Appendix 1 for definition of variables), where shadowing effects appear. In the region of valence quarks and nuclear effects ( $x_b > 0.1 - 0.2$ ) the most reliable data presently available are from the SLAC E139<sup>[5,6]</sup> (see fig. 1) and E140<sup>[7]</sup> experiments.

New precise data in the valence quark region are necessary to determine the real  $A$ -dependence of the ratio between bound and free nucleon structure functions  $F_2(x_b)$  which is not completely defined by the SLAC data. From the nuclear physics point of view, a measurement on a fundamental and still unexplored nucleus like  ${}^3\text{He}$  would be of great interest because calculations are better verified for this nucleus. In addition, a reliable measurement of nuclear medium effects in the structure function  $R(x_b)$  could shed light on a more detailed understanding of hadron structure.

With at least a 6 GeV beam the intermediate scaling region ( $0.1 < x_b < 0.6$ ) can be readily accessible at CEBAF. The physics program we propose is complementary to that already approved in Hall C to study the correlations and multi-quark states in nuclei for the  $x_b > 1$  region<sup>[8]</sup>.

## PHYSICS OVERVIEW

### Proton and Neutron Structure Functions

To get detailed information of nuclear medium effects in structure functions it is necessary to measure them on free and bound nucleons in the same kinematical and experimental conditions. This minimizes systematic errors in ratios or differences and takes properly into account proton and neutron differences in non-isoscalar nuclei (like in the case of  $^3\text{He}$ ). We will thus perform a precise measurement of the proton and neutron structure functions ( $F_2^p(x_b)$  and  $F_2^n(x_b)$ ), which gives direct information about the momentum distributions of valence and sea quarks inside the nucleon. In fig. 2 the available data<sup>[9]</sup> <sup>[10]</sup> <sup>[11]</sup> on the ratio  $F_2^n/F_2^p$  measured with deuterium and hydrogen targets are shown. The extraction of the neutron structure function is quite well understood now, with a maximum correction of about 2% due to Fermi motion in deuterium<sup>[12]</sup> for  $x_b < 0.7$ .

The hypothesis of similar sea-quark distributions in proton and neutron is supported by experimental data in the low  $x_b$  region ( $x_b < 0.01$ ), where the ratio  $F_2^n/F_2^p$  goes to 1 and there is little evidence for shadowing in deuteron as suggested by real photon experiments. At high values of  $x_b$  ( $x_b > 0.7$ ) the ratio goes approximately to the value  $(\frac{q_{down}}{q_{up}})^2 = 0.25$  obtained in a simple quark model considering the contribution of the double valence quarks only; nevertheless in this region both statistic and systematic errors are large and the Fermi correction of the deuteron structure function becomes important.

In the intermediate valence quark region ( $0.1 < x_b < 0.6$ ) where we plan to study, there is a 10-20% discrepancy among data that can only partially be explained by  $Q^2$  scaling violation. Next to leading order calculation in QCD with the inclusion of target mass effects predicts a  $[\ln Q^2]$  behaviour with a slope between 0 and -0.01 in the intermediate  $x_b$  range, while the slope for each data set is systematically bigger. (-0.015 for the SLAC data<sup>[9]</sup>; -0.019 for the combined SLAC and NMC data<sup>[11]</sup>; -0.02 for the combined SLAC and BCDMS data<sup>[9]</sup>). For this reason, a precise measure of this ratio at a given  $Q^2$  is of fundamental importance for the measurement of structure functions in non-isoscalar nuclei.

The integral of the difference of structure functions,  $\int_0^1 (F_2^p - F_2^n) dx_b/x_b$ , has been used to calculate the Gottfried sum rule. The experimental value of about 0.24<sup>[13]</sup> (see fig. 3) disagrees significantly with respect to the quark-parton model expectation of 1/3, providing strong evidence that SU(2) flavor symmetry is broken by the sea quark distributions of the nucleon. From the NMC<sup>[13]</sup> experimental values we see that 60% of the integral comes from data in the intermediate region of  $x_b$  (0.1 to 0.6) where the experimental errors are large. Hence a precise measurement in this region will better help define the discrepancy between theoretical predictions and experimental findings.

## Structure Function $F_2(x_b)$ in Nuclei

The difference of quark distributions in free and bound nucleons can be due to the partial deconfinement of quarks in nuclei and related to such effects as quark exchange, swelling of nucleons, formation of multi-quark bags and  $Q^2$  rescaling effects caused by the increase of the radius of confinement ( see ref.[14-17] ). Moreover the quark distributions in nuclei can be deformed due to Fermi motion, removal energy and binding effects, commonly referred to as "standard" nuclear effects. ( see ref. [12,18,19] ).

It has been argued that when relativistic effects are consistently taken into account by considering the so called flux factor in the normalization of the relativistic spectral function [17], the effects of nucleon binding energy  $E$  and kinetic energy  $T$  are strongly reduced. Also nucleonic correlations, which increase in a significant way  $E$  and  $T$  in comparison with Hartree-Fock models, are not able to explain definitively the data for  $x_b \geq 0.5$ , so that non-nucleonic degrees of freedom or bound nucleon modifications[12] should also be considered.

There are different models that postulate an increase of quark confinement radius inside the nucleus. For instance this can be explained by introducing quark deconfinement because of the admixture of multi-quark states. In the framework of this model[14,15], the ratio of nuclear and deuterium structure functions can be written:

$$\frac{F_2^A}{F_2^D} = 2 \frac{(1-w)F_2^N + wF_2^B}{F_2^D}$$

where  $F_2^N$  is the nucleon structure function corrected for Fermi motion,  $F_2^D$  is the deuteron structure function,  $F_2^B$  is the cluster structure function and  $w$  the cluster relative probability; this probability increases from 10% in  ${}^4\text{He}$  to 30% in  ${}^{56}\text{Fe}$ .

A more systematic and precise study of the nuclear structure function is needed to improve and complete the SLAC data. In fact the SLAC data are not able to disentangle the  $A$  behaviour of the ratio  $\sigma^A/\sigma^D$  between a power law  $\sigma^A/\sigma^D = cA^\alpha$  and a nuclear density law  $\sigma^A/\sigma^D = a(1 + b\rho(A))^{[6]}$  as suggested for instance by multi-quark state models. As shown in fig. 4 both fits are consistent with data within experimental errors but they are not able to reproduce the value equal to one for the deuteron (which is included as a data point in the fits). It is therefore possible that a nuclear density fit could be better verified in light nuclei where the density changes very quickly and with a non-monotonic law rather than in medium and heavy nuclei.

It is important to point out that whereas  $Q^2$  scaling violations have been clearly shown in the measurements of the absolute values of structure function  $F_2$ , no significant  $Q^2$  dependence was ever found in the ratio of structure functions for nuclei, allowing us to perform this measurement in the region of modest values of  $Q^2$ .

## Structure Function $F_2(x_b)$ in ${}^3\text{He}$ and ${}^4\text{He}$

Data are presently available for several nuclei from  ${}^4\text{He}$  to  ${}^{197}\text{Au}$  and the EMC effect is well evident for all. In particular in the region of  $x_b \sim 0.5 - 0.6$  the size of this effect in  ${}^4\text{He}$  is 40 to 50% of the effect in the heaviest target. Unfortunately no data are yet available on  ${}^3\text{He}$  that might help to understand this behaviour in very light nuclei. Many nucleonic and non nucleonic interpretations are able to reproduce the data in heavy nuclei, but none can be used to draw definite conclusions. It should be stressed, however, that those interpretations which are able to reproduce the data for heavy nuclei are generally parameter dependent as far as nuclear structure is concerned. Therefore a careful measurement in few body systems becomes essential. The fact that the  ${}^3\text{He}$  spectral function is exactly known and the one for  ${}^4\text{He}$  can be computed much better than in heavier nuclei suggests that data from these two nuclei should provide a good tool for discriminating between different theories.

The pure nucleonic contribution can be analyzed in terms of momentum distributions and spectral functions employing realistic nucleon-nucleon interactions for few-nucleon systems: in fig. 5 the result of such calculations for  ${}^3\text{He}$  and  ${}^4\text{He}$  is presented with the inclusion of relativistic effects (the so called flux factor).<sup>[12]</sup>

A very different approach shows that quark exchange between static nucleons (no "standard" nuclear effects) can be precisely evaluated and give an overall non-negligible effect of a few percent in the ratio for a relative dilute nucleus like  ${}^3\text{He}$ .<sup>[20]</sup> In fig. 6 the effect has been plotted for two different nucleon radii and compared with a rescaling prediction. (It is worth mentioning that for non-isoscalar nuclei  $F_2^D$  should be replaced by  $ZF_2^p + NF_2^n$ ). Figures 5 and 6 also contain the projected data in the proposed experiment showing that it will be possible to measure small effects like those predicted for  ${}^3\text{He}$  and to distinguish clearly between the two Helium isotopes.

It is also clear that the possible formation of a multi-quark cluster bag inside the nucleus<sup>[15]</sup> can be easily checked by comparing the structure function measured for the two Helium isotopes because of the very different probability of finding 6-quark, 9-quark or 12-quark clusters.

## Structure Function $R(x_b)$ in Nuclei

The structure function  $R(x_b)$  is expressed by the ratio  $R(x_b) = \sigma_L(x_b)/\sigma_T(x_b)$ . This ratio vanishes in the quark parton model according to the Callan- Gross relation due to the spin 1/2 of quarks at high  $Q^2$  values. In the region of low and moderate  $Q^2$ , possible non-zero contributions could arise from kinematical mass effects, internal quark transverse momenta and perturbative QCD corrections. Nevertheless, taking all these effects into account, theory fails to reproduce experimental data for  $R^p$  and  $R^D$  in the region of  $x_b > 0.2$  and  $Q^2 < 6(\text{GeV}/c)^2$  where  $R(x_b)$  seems consistent with an almost constant value of about 0.2.<sup>[7]</sup> In order to explain this big discrepancy, a very large contribution of higher order twist effect due to quark-gluon correlation is required.<sup>[21]</sup>

A possible and non-negligible contribution to  $R(x_b)$  in this kinematical domain is also suggested by a quark-diquark configuration of the nucleon which introduce a spin-0 constituent that could be coupled longitudinally to the virtual photon. <sup>[22,23]</sup> These models predict that diquark effects increase for increasing  $x_b$  and decreasing  $Q^2$  and that  $R$  could be affected by the nuclear medium. Fig. 7 shows the prediction of a simple diquark model <sup>[22]</sup> in comparison with the QCD prediction range (with target mass correction) and with experimental data at moderate  $Q^2$ .<sup>[7]</sup>

Sparse information is presently available about the possible variation of the structure function  $R(x_b)$  in nuclei. In this case the interesting observable is the difference  $(R^A(x_b) - R^D(x_b))$  which can be directly determined from measured cross sections  $\sigma^A$  and  $\sigma^D$  with a linear fit in the Rosenbluth plane:

$$\frac{\sigma^A}{\sigma^D} = \frac{\sigma_T^A}{\sigma_T^D} [1 + \epsilon'(R^A - R^D)]$$

where  $\epsilon' = \epsilon/(1 + \epsilon R^D)$ . Fig. 8 shows a typical expected Rosenbluth plot with reasonable values. Fig. 9 shows the only data for  $(R^A(x_b) - R^D(x_b))$  from SLAC E140.<sup>[7]</sup> An overall  $x_b$ -average of all data points is compatible with no difference within the quoted error; nevertheless an  $x_b$ -dependence of this difference should not be excluded, because the data show a possible large increase of about 0.1 (which corresponds to a 50% variation) when going from low to intermediate  $x_b$  values, where possible diquarks effects could show up. Our projected data for the same nucleus, indicate that we will be able to measure quite well variations bigger then 0.025 (which is about a 10% effect). A 50% variation in  $(R^A - R^D)$  implies a non-negligible difference of about 5% between  $\sigma^A/\sigma^D$  and  $F_2^A/F_2^D$

An indication of the possible variation of  $R$  in nuclei was observed in SLAC E139<sup>[5]</sup> in the region  $0.3 < x_b < 0.7$ , which is the region of possible diquark effects (see fig. 10). Due to the large error bars no definitive conclusion could be drawn also for this measurement, but an increase of  $R$  with mass number  $A$  is not excluded and, as shown, could be much better determined by the proposed experiment. Any  $A$  dependence of  $(R^A - R^D)$  shouldn't be ascribed to a trivial shadowing effect as this is completely negligible in the whole range of the proposed measurement<sup>[24]</sup>.

## PROPOSED EXPERIMENT

### New possibilities at CEBAF

An exact kinematic reconstruction, through a better than 0.1% measurement of the incoming and scattered electron energies  $E$  and  $E'$  and a scattering angle determination of better than 1 mrad, is needed for a precise measurement of the structure functions. A precise determination of the spectrometer acceptance and efficiency and a high  $\pi/e$  rejection factor (of the order of  $10^4 : 1$ ) are also important.

All these requirements should be satisfied by the high quality electron beam used together with the HALL A HRS spectrometers at CEBAF. In comparison with the previous SLAC experiments E139 and E140 one can expect an increase in sensitivity of a factor 100 due to solid angle, momentum acceptance and beam intensity, leading to a significant improvement of nearly an order of magnitude in the statistical error, which was the major contribution of the total error in the SLAC data.

We can also expect a non-negligible improvement of the systematic error through a better determination of the incoming beam energy and angle, which were main sources of systematic error of the SLAC measurements.

The availability of high quality and high power cryogenic targets will allow to measure, for the first time and in the same kinematical and experimental conditions, nuclear medium effects in the few-nucleon systems. Furthermore the vertex reconstruction capability of HRS would allow a good rejection of cryogenic target wall backgrounds.

We propose to measure the inclusive cross sections on  $^1\text{H}$ ,  $^2\text{H}$ ,  $^3\text{He}$ ,  $^4\text{He}$ ,  $^7\text{Li}$ ,  $^{12}\text{C}$ ,  $^{56}\text{Fe}$ ,  $^{118}\text{Sn}$  in several kinematic regions in order to determine the respective structure functions  $F_2(x_b)$  and  $R(x_b)$ . We will detect the scattered electrons with one HRS spectrometer and use the other one at fixed angle to monitor the luminosity. We could also explore the possibility of using both spectrometers for data taking to reduce the time required to accumulate data, if needed.

### Choice of Kinematics

To determine the structure functions  $F_2(x_b)$  and  $R(x_b)$  from the cross sections, a Rosenbluth separation with at least two beam energies will be necessary. With a 6 GeV maximum beam energy, it would be convenient to use the 5th and 4th beam recirculation corresponding to 6 and 4.8 GeV respectively. Moreover a third intermediate energy (5.4 GeV) will be used for a better slope determination (see fig. 8). In this case, using the almost universal standard cuts, the available kinematic region for deep inelastic processes is shown in fig. 11 and is defined approximately by the area enclosed by the line  $W \geq 2$  GeV (resonance constraint), the line  $Q^2 \geq 1$  GeV<sup>2</sup> (scaling constraint) and the line  $\nu \leq 4.1$  GeV ( $y_{max} = \nu_{max}/E_{min} = 0.85$  due to radiative correction constraint). The  $x_b$  range to be explored is 0.1 to 0.6, where for each  $x_b$  point the maximum  $Q^2$  (and  $\nu$ ) is selected to minimize possible higher twist effects in the ratio of structure functions. Target mass corrections can be properly taken into account considering the Nachtmann scaling variable  $\xi$  instead of the Bjorken variable  $x_b$ .

## Target Requirements

For the proposed measurement several kinds of target will be required; specifically:

- liquid hydrogen and deuterium targets, operating at 20 K;
- high pressure (70 Atm)  $^3\text{He}$  and  $^4\text{He}$  gas targets, operating at 20 K;
- solid targets for other nuclei.

All these targets have to operate with a beam current of 60  $\mu\text{A}$ , which correspond to a power dissipation of about 300 Watt for a hydrogen or deuterium target of 15 cm. Therefore beam position rastering or direct cooling of the targets will be necessary. Moreover the continuous duty-factor of the beam will strongly reduce local hot spots that could occur when using low duty-factor beams with high instantaneous currents.

We therefore propose the following arrangement for the targets:

- 4 measurements with cryogenic targets ( $^1\text{H}$ ,  $^2\text{H}$ ,  $^3\text{He}$  and  $^4\text{He}$ ) with 1% radiation lengths  $X_0$  and 60  $\mu\text{A}$  beam.
- 4 measurements with solid targets ( $^7\text{Li}$ ,  $^{12}\text{C}$ ,  $^{56}\text{Fe}$ ,  $^{118}\text{Sn}$ ) with 4%  $X_0$  and 60  $\mu\text{A}$  beam.

Moreover a good check of radiative corrections could be performed by comparing data taken with solid targets of various well known thicknesses. Due to the longitudinal acceptance and the vertex reconstruction capability of the spectrometer a possible simultaneous use of solid targets could also be considered.

## Counting Rate Estimates and Time Request

Count rate estimates were based on the following consideration. Scattering cross section can be written as:

$$\sigma = \sigma_M \left[ \frac{F_2(x_b, Q^2)}{\nu} + \frac{2F_1(x_b, Q^2)}{M} \tan^2\left(\frac{\Theta}{2}\right) \right]$$

where  $\sigma_M$  is the Mott cross section.

Quarks being fermions of spin 1/2, one can then assume, for counting rate purposes only and at intermediate values of  $x_b$ , the Callan-Gross law  $F_2 = 2x_b F_1$ . Also assuming the longitudinal contribution to the cross section to be small, one gets:

$$\sigma = \sigma_M \left[ \frac{1}{\nu} + \frac{2\nu}{Q^2} \tan^2\left(\frac{\Theta}{2}\right) \right] F_2(x_b, Q^2)$$

where the structure function in the x range considered can be fitted with the formula:

$$F_2^p(x_b, Q^2) = 2.2x_b^{0.7}(1 - x_b)^3$$

This approximate formula, which we have used to calculate counting rates, has been compared with the SLAC data on hydrogen in kinematics similar to those we propose using at CEBAF ( $E \leq 6$  GeV,  $x_b = 0.1-0.6$ ) and we have found it to reproduce the measured data to within 10-20%. In fig. 12 we show curves of constant cross section (in nb  $\text{GeV}^{-1} \text{sr}^{-1}$ ) for a 6 GeV beam, calculated with this formula. We plan

to do a more detailed MonteCarlo simulation for these kinematics. The cross section on neutron has been estimated assuming  $\sigma_n = (1 - 0.8x_b)\sigma_p$ , while the cross sections on nuclei were computed assuming no nuclear medium effects.

$x_b$	$\xi$	$Q^2$ (GeV/c) <sup>2</sup>	$W$ (GeV)	$\theta$ (deg)	$\epsilon$	$\sigma$ (nb/GeV/sr)	counts (s <sup>-1</sup> )
.10	.099	.77	2.79	14.9	.560	67.8	12400
.15	.148	1.15	2.73	18.3	.553	33.5	6150
.20	.196	1.54	2.65	21.2	.546	19.1	3510
.25	.243	1.92	2.58	23.7	.538	11.7	2150
.30	.290	2.31	2.50	26.0	.531	7.49	1370
.35	.337	2.69	2.43	28.1	.524	4.89	896
.40	.383	3.08	2.34	30.1	.517	3.21	590
.45	.429	3.46	2.26	32.0	.510	2.11	388
.50	.474	3.85	2.17	33.8	.503	1.38	253
.55	.519	4.23	2.08	35.5	.496	.883	162
.60	.564	4.61	2.00	37.1	.489	.551	101

**Table 1a.** Kinematic parameters for  $E_0 = 6$  GeV ( $E' = 1.9$  GeV and  $\nu = 4.1$  GeV); cross sections and rate are calculated with the formula and the assumptions described in the text.

$x_b$	$\xi$	$Q^2$ (GeV/c) <sup>2</sup>	$W$ (GeV)	$\theta$ (deg)	$\epsilon$	$\sigma$ (nb/GeV/sr)	counts (s <sup>-1</sup> )
.10	.099	.77	2.79	27.7	.265	18.4	1240
.15	.148	1.15	2.72	34.1	.255	9.08	614
.20	.196	1.54	2.65	39.6	.245	5.16	349
.25	.243	1.92	2.58	44.5	.235	3.16	213
.30	.290	2.31	2.50	49.0	.226	2.01	136
.35	.337	2.69	2.43	53.2	.216	1.30	88.2
.40	.383	3.08	2.34	57.2	.207	.855	57.8
.45	.429	3.46	2.26	61.0	.198	.560	37.9
.50	.474	3.85	2.17	64.7	.188	.364	24.6
.55	.519	4.23	2.08	68.3	.180	.232	15.7
.60	.564	4.61	2.00	71.8	.171	.144	9.75

**Table 1b.** Kinematic parameters for  $E_0 = 4.8$  GeV ( $E' = 0.7$  GeV and  $\nu = 4.1$  GeV); cross sections and rate are calculated with the formula and the assumptions described in the text.

$x_b$	Cryogenic Targets				Solid Target Sets			
	$^1\text{H}$	$^2\text{H}$	$^3\text{He}$	$^4\text{He}$	$^7\text{Li}$	$^{12}\text{C}$	$^{56}\text{Fe}$	$^{118}\text{Sn}$
.10	<0.1	<0.1	<0.1	<0.1	<0.1	<0.1	<0.1	<0.1
.15	<0.1	<0.1	<0.1	<0.1	<0.1	<0.1	<0.1	<0.1
.20	<0.1	<0.1	<0.1	<0.1	<0.1	<0.1	<0.1	<0.1
.25	<0.1	<0.1	<0.1	<0.1	<0.1	<0.1	<0.1	<0.1
.30	<0.1	<0.1	<0.1	<0.1	<0.1	<0.1	<0.1	<0.1
.35	<0.1	<0.1	<0.1	<0.1	<0.1	<0.1	<0.1	<0.1
.40	<0.1	<0.1	<0.1	<0.1	<0.1	<0.1	<0.1	<0.1
.45	<0.1	<0.1	<0.1	<0.1	<0.1	<0.1	<0.1	0.15
.50	0.11	<0.1	0.11	<0.1	<0.1	<0.1	0.15	0.24
.55	0.18	0.11	0.17	0.14	<0.1	<0.1	0.24	0.38
.60	0.28	0.18	0.29	0.24	<0.1	0.13	0.41	0.65
Subtotal	1.4	1.2	1.4	1.3	1.1	1.1	1.6	2.1
Total	5.3				5.9			

**Table 2a.** Time required in hours for 0.3% statistics for each data point (100,000 counts) for  $E_0 = 6.0$  GeV ( $E' = 1.9$  GeV and  $\nu = 4.1$  GeV).

$x_b$	Cryogenic Targets				Solid Target Sets			
	$^1\text{H}$	$^2\text{H}$	$^3\text{He}$	$^4\text{He}$	$^7\text{Li}$	$^{12}\text{C}$	$^{56}\text{Fe}$	$^{118}\text{Sn}$
.10	<0.1	<0.1	<0.1	<0.1	<0.1	<0.1	<0.1	<0.1
.15	<0.1	<0.1	<0.1	<0.1	<0.1	<0.1	<0.1	0.1
.20	<0.1	<0.1	<0.1	<0.1	<0.1	<0.1	0.1	0.15
.25	0.13	<0.1	0.12	<0.1	<0.1	<0.1	0.16	0.25
.30	0.21	0.12	0.18	0.15	<0.1	<0.1	0.26	0.40
.35	0.31	0.18	0.29	0.24	<0.1	0.13	0.39	0.63
.40	0.48	0.29	0.49	0.37	0.11	0.20	0.63	0.99
.45	0.73	0.45	0.73	0.58	0.17	0.32	0.98	1.54
.50	1.13	0.71	1.10	0.92	0.26	0.51	1.54	2.43
.55	1.77	1.11	1.70	1.44	0.41	0.80	2.41	3.84
.60	2.85	1.87	2.88	2.42	0.69	1.34	4.06	6.46
Subtotal	7.9	5.1	7.8	6.5	2.2	3.8	10.7	16.9
Total	27.3				33.6			

**Table 2b.** Time required in hours for 0.3% statistics for each data point (100,000 counts) for  $E_0 = 4.8$  GeV ( $E' = 0.7$  GeV and  $\nu = 4.1$  GeV).

To estimate the count rates we have assumed a 60  $\mu\text{A}$  beam current, a 1%  $X_0$  hydrogen target (total luminosity of about  $1.4 \cdot 10^{38} \text{ cm}^{-2} \text{ s}^{-1}$ ), a 7.0 msr solid angle and a momentum bite  $\Delta p/p$  of 10% for the spectrometer. In table 1 are listed the kinematic parameters and the counting rates for the proposed measurement on the hydrogen target for the maximum and minimum beam energy.

We have then scaled these rates with the luminosities available for the other targets with the previously described simple assumptions about their respective cross sections to obtain their rates. In Table 2 we list the time required in hours to accumulate 0.3% statistics (100,000 events) for each  $x_b$  experimental point. In most cases especially at 6 GeV the time required is less than 6 minutes (0.1 hours) to acquire the requisite statistics and we have used this as the minimum time for each data point. In Table 3 we give the details of the time requested for the cryogenic and solid targets and for the three sets of kinematics. Even though the actual time for data taking is only about 108 hours, a considerable overhead in time is necessary for changing targets, angles and energy. We also reserve sufficient time for various calibration runs which include time for radiative correction checks, rate effects, empty target runs etc.. Taking all of this into account, we request a cumulative beam time of 454 hours for all the nuclei proposed.

**Table 3.** Cumulative time request in hours

	Cryogenic Targets	Solid Targets
1) <u>Kinematics at 6 GeV</u>		
Data taking time (see Table 2)	5	6
Angle changes (4 hr/target)	16	16
Energy changes (4 hr/target)	16	16
2) <u>Kinematics at 5.4 GeV</u>		
Data taking time	16	20
Angle changes (4 hr/target)	16	16
Energy changes (4 hr/target)	16	16
3) <u>Kinematics at 4.8 GeV</u>		
Data taking time (see Table 2)	27	34
Angle changes (4 hr/target)	16	16
Target changes (8 hr/cryotargets) (2 hr/solid targets)	32	8
4) <u>Calibration Runs</u>	48	48
Radiative corr. checks, Empty target runs, rate effects...		
5) Setup Time	24	24
Total	232	222

## Systematic and Statistical Errors Estimates

An estimate of the systematic errors could be done in comparison with the previous SLAC experiment by comparing expected beam, targets and spectrometer performances. In table 4 we give a comparison of the main sources of error and how they propagate in the relevant variables for the case of  ${}^4\text{He}$  and  ${}^{56}\text{Fe}$  targets. It is important to note that the typical main sources of error that affect total cross section  $\sigma$ , like acceptance, absolute beam current, detector efficiency, radiative corrections, almost cancel and vanish in the measured quantities. They only influence the determination of absolute structure functions.

The comparison has been made with E139 for the  $\sigma^A/\sigma^D$  measurement and with E140 for the  $R^A - R^D$  measurement. As is seen, we expect a total point to point error of about 0.5% for  $\sigma^A/\sigma^D$  and of 0.025 for  $R^A - R^D$  with an improvement of a factor 3 in the comparison with SLAC, mainly due to the very low statistical errors of the proposed experiment.

**Table 4.** Sources and typical magnitude of the systematic uncertainties, as well as their effects on cross section ratios and structure function differences of the proposed CEBAF experiment compared to the previous SLAC experiments E139 and E140.

Source of Error	SLAC	SLAC	CEBAF	$\sigma^{Fe}/\sigma^D$		$\sigma^{He}/\sigma^D$		$R^{Fe} - R^D$	
	E139	E140		E139	CEBAF	E139	CEBAF	E140	CEBAF
Incident Energy*	0.1%	0.1%	0.01%	0.3%	0.03%	0.3%	0.03%	0.014	0.002
Beam Angle	0.2 mr	0.05 mr	0.03 mr	0.6%	0.1%	0.6%	0.1%	0.004	0.002
Beam Current*	0.2%	0.2%	0.2%	0.1%	0.1%	0.1%	0.1%	0.004	0.004
D target density*	0.5%	0.3%	0.3%	0.5%	0.3%	0.5%	0.3%	0.014	0.014
He Target density*	1.4%		0.5%			1.4%	0.5%		
Scattered Energy*	0.05%	0.05%	0.01%	0.1%	0.02%	0.1%	0.02%		
Acceptance vs. $\theta$	0.1%	0.1%	0.1%	0.1%	0.1%			0.004	0.004
Total Systematic (pt. to pt.)				0.85%	0.35%	1.6%	0.6%	0.021	0.015
Total Statistics				1.2%	0.25%	1.5%	0.25%	0.060	0.020
Total (pt. to pt.)				1.5%	<b>0.45%</b>	2.2%	<b>0.65%</b>	0.065	<b>0.025</b>
Target Length				0.8%	0.5%	2.1%	1.0%		
Rad. corrections	1.0%	1.0%	1.0%	0.5%	0.5%	0.5%	0.5%	0.015	0.015
Total (target to target)				1.0%	<b>0.7%</b>	2.2%	<b>1.1%</b>	0.015	<b>0.015</b>

\* Fluctuations of nominal value

## CONCLUSIONS

Unpolarized structure functions of free and bound nucleons can be measured with the CEBAF 6 GeV beam in the valence quark region. An improvement on the precision of actual data for  $F_2$ , the measurements on non isoscalar nuclei and the measurement of  $R$  will provide a tool for discriminating the standard nuclear models from more exotic ones. In the event of a future upgrade of CEBAF energies to 10 GeV, these measurements can be naturally extended to a larger interval in  $x_b$ .

This physics program can also be extended to future measurements of polarized structure functions when the polarization of the beam and of the targets become available. In particular, we point out that about 75% of the integral of the polarized structure function of the proton,  $\int_0^1 g_1^p(x_b) dx_b$ , which does not agree with the prediction of the Ellis-Jaffe sumrule, is determined in the region of intermediate  $x_b$  value ( $0.1 \leq x_b \leq 0.7$ ) which is accessible with a 6 GeV beam and that the measured asymmetry  $A_1^p$  is almost  $Q^2$  independent in the range  $1 \text{ (GeV/c)}^2 \leq Q^2 \leq 100 \text{ (GeV/c)}^2$ .

## REFERENCES

- 1) J.J. Aubert et al., *Phys. Lett.* 123B (1983) 275.
- 2) A.C. Benvenuti et al., *Phys. Lett.* B189 (1987) 483.
- 3) P. Amaudruz et al., CERN-PPE/91-52.
- 4) M.R. Adams et al., *Phys. Rev. Lett.* 68 (1992) 3266.
- 5) R.G. Arnold et al., *Phys. Rev. Lett.* 52 (1984) 727.
- 6) J. Gomez et al., *Phys. Rev. D* 49 (1994) 4348 and J. Gomez, Ph.D. thesis, American University, 1987 (unpublished).
- 7) S. Dasu et al., *Phys. Rev. D* 49 (1994) 5641.
- 8) B. Filippone and D. Day, Spokespersons, CEBAF PR-89-008.
- 9) L. W. Whitlow, Ph. D. thesis, SLAC-357 (1990); and L.W. Whitlow et al., *Phys. Lett. B* 282 (1992) 475.
- 10) A.C. Benvenuti et al., *Phys. Lett.* B237 (1990) 599.
- 11) D. Allasia et al., CERN-PPE/90-103.
- 12) C. Ciofi degli Atti and S. Liuti, *Phys. Rev. C* 41 (1990) 1100; and *Phys. Rev. C* 44, Rapid Communications.
- 13) M. Arneodo et al., CERN-PPE/94-32.
- 14) F.E. Close et al, *Phys. Rev. D* 31 (1985) 1004.
- 15) L.A. Kondratyuk and M.Zh.Shmatikov, *Z. Phys. A* 321(1985) 301.
- 16) E.L. Berger et al., *Ann. Rev. Nucl. Part. Sci.* 37 (1987) 463.
- 17) L.L. Frankfurt and M.I.Strikmann, *Phys. Rep.* 160 (1988) 236.
- 18) A. Bodek et al., *Phys. Rev. D* 23 (1981) 1071.
- 19) S.V. Akulinichev et al., *Phys. Rev. Lett.* 55 (1985) 2239.
- 20) P. Hoodbhoy and R.L. Jaffe *Phys. Rev. D* 35 (1987) 113.
- 21) J.L. Miramontes et al., *Phys. Rev. D* 40 (1989) 2184.
- 22) L.F. Abbott et al., *Phys. Lett. B* 88 (1979) 157.
- 23) S. Ekelin and S. Fredriksson, *Phys. Lett. B* 162 (1985) 374.
- 24) V. Barone et al., *Phys. Lett. B* 304 (1993) 176.

## APPENDIX 1

### Variables definition

$E_0$ : Beam energy.

$E'$ : Recoil electron energy.

$\Theta$ : Electron scattering angle.

$Q$ : 4-momentum transfer.

$$Q^2 = 4E_0 E' \sin^2(\Theta/2)$$

$\nu$ : Energy transfer.

$W$ : Invariant mass of the hadronic final state.

$$W^2 = [M^2 + (2M\nu - Q^2)]$$

$x_b$ : Bjorken scaling variable.

$$x_b = Q^2/2M\nu$$

$\xi$ : Nachtmann scaling variable.

$$\xi = \left[ \frac{2x_b}{1 + \sqrt{1 + \frac{4M^2 x_b^2}{Q^2}}} \right]$$

$\sigma$ : Differential cross section expressed in  $d\Omega dQ^2$ .

$$\sigma = \Gamma [\sigma_T(x, Q^2) + \epsilon \sigma_L(x, Q^2)]$$

$$\sigma = \sigma_M F_2 \left[ 1 + \frac{1 - \epsilon}{\epsilon} \frac{1}{1 + R} \right]$$

$\Gamma$ : Virtual photon flux with transverse polarization.

$$\Gamma = \frac{\alpha E'}{4\pi Q^2 E_0} \left[ \frac{(W^2 - M^2)}{2M(1 - \epsilon)} \right]$$

$\epsilon$ : Relative virtual photon flux with longitudinal polarization.

$$\epsilon = \left[ 1 + 2 \left( 1 + \frac{\nu^2}{Q^2} \right) \tan^2 \left( \frac{\Theta}{2} \right) \right]^{-1}$$

$\sigma_M$ : Mott cross section.

$$\sigma_M = \frac{4\alpha^2 E'^2}{Q^4} \cos^2 \left( \frac{\Theta}{2} \right)$$

## Figure Captions

**Fig 1.**  $\sigma^A/\sigma^D$  as function of  $x_b$  for various nuclei (from ref.<sup>[6]</sup>).

**Fig 2.**  $F_2^n/F_2^p$  as function of  $x_b$  (from ref.<sup>[11]</sup>).

**Fig 3.** The difference  $F_2^p - F_2^n$  and the Gottfried Sum Rule at  $Q^2 = 4G\epsilon V^2$ . (data from ref.<sup>[13]</sup>). The extrapolated result  $S_G$  is indicated by the bar. The simple quark-parton model (QPM) prediction is also shown.

**Fig 4a.** Ratios  $(\sigma^A/\sigma^D)^{[6]}$  versus atomic weight  $A$  at  $x_b=0.6$ . Solid line is a model fit of the data as a power law of  $A$ . Also shown are the CEBAF projected data with total errors (statistical+total systematic).

**Fig 4b.** Ratios  $(\sigma^A/\sigma^D)^{[6]}$  versus nuclear density at  $x_b = 0.6$ . Solid line is a model fit of the data as a linear dependence of nuclear density.

**Fig 5.**  $^3\text{He}$  and  $^4\text{He}$  predictions from pure nucleonic theory (from ref. <sup>[12]</sup>). Also shown are the  $^4\text{He}$  SLAC E139 previous data and the CEBAF  $^3\text{He}$  and  $^4\text{He}$  projected data with total errors (statistical and point to point systematic).

**Fig 6.**  $^3\text{He}$  prediction from the quark-exchange model for two nucleon radii ( $r$ ) and from a rescaling model (from ref. <sup>[20]</sup>). Also shown are the CEBAF  $^3\text{He}$  and projected data with total errors (statistical and point to point systematic).

**Fig 7.** Structure Function  $R(x_b)$  as function of  $x_b$  for intermediate values of  $Q^2$  <sup>[7]</sup>. The dashed area is the range of QCD calculations including target mass effects, while dashed curve is the prediction of a diquark model neglecting all other contributions<sup>[22]</sup>.

**Fig 8.** Typical expected determination of the quantity  $(R^A - R^D)$  for the CEBAF proposed experiment, with reasonable numbers and total errors.

**Fig 9.**  $(R^A - R^D)$  versus  $x_b$  measured by SLAC E140<sup>[7]</sup> compared with our projected data. Error bars are total error (statistical + point to point systematic).

**Fig 10.**  $R^A$  versus atomic weight  $A$  measured by SLAC E139<sup>[5]</sup> compared with our projected data for  $(R^A - R^D)$ . Error bars are total error (statistical + total systematic).

**Fig 11.** Kinematic plane for inclusive electron scattering ( $e, e'$ ) with a 6 GeV maximum beam energy. Close circles indicate the kinematic points for this proposal for measuring  $\sigma$ ,  $F_2$  and  $R$ .

**Fig 12.** Curves for constant cross section (in nb  $GeV^{-1} sr^{-1}$ ) at 6 GeV.

- E139 (Be, C, Al, Ag, Au)
- + BCDMS (N, Fe)
- ◊ E61 (Be, Al, Cu, Au)
- ◻ E87 (Al, Fe)
- × E140 (Fe, Au)
- △ EMC-NA2' (C, Cu)

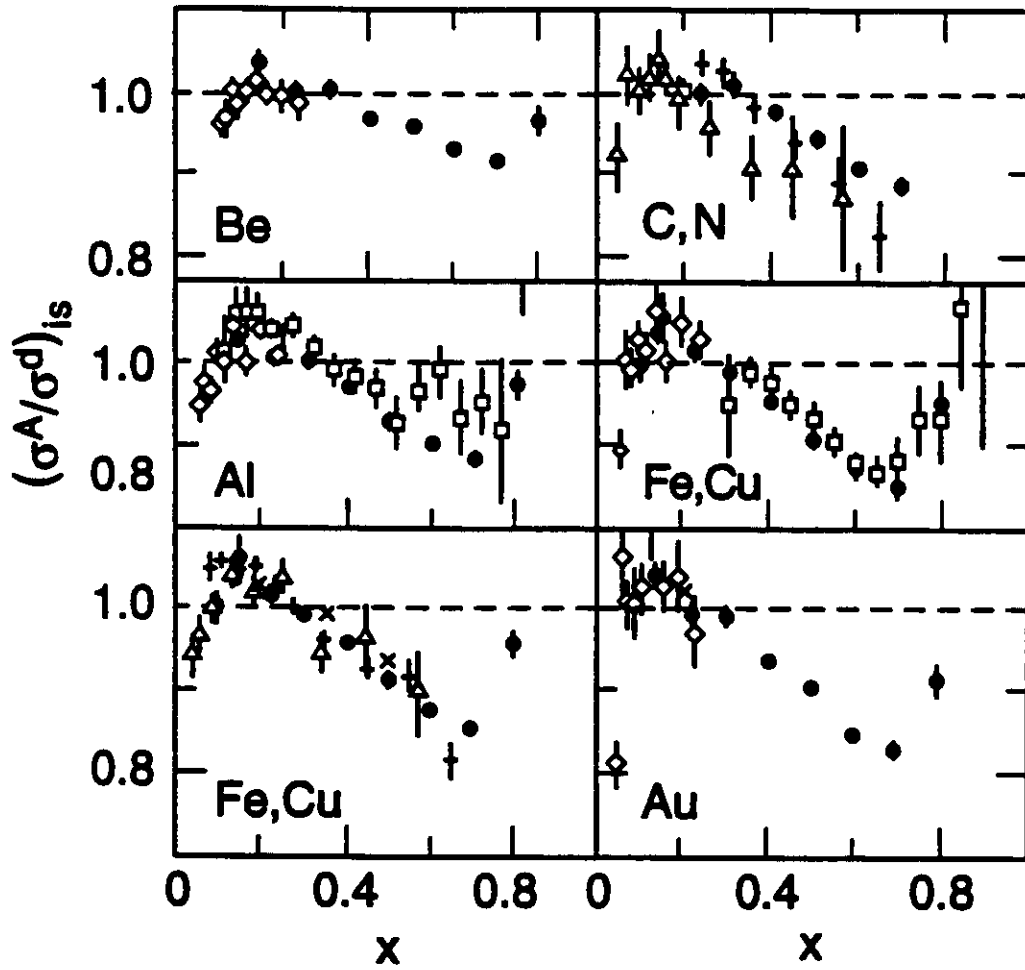


Fig 1.  $\sigma^A/\sigma^D$  as function of  $x_b$  for various nuclei (from ref.<sup>[6]</sup>).

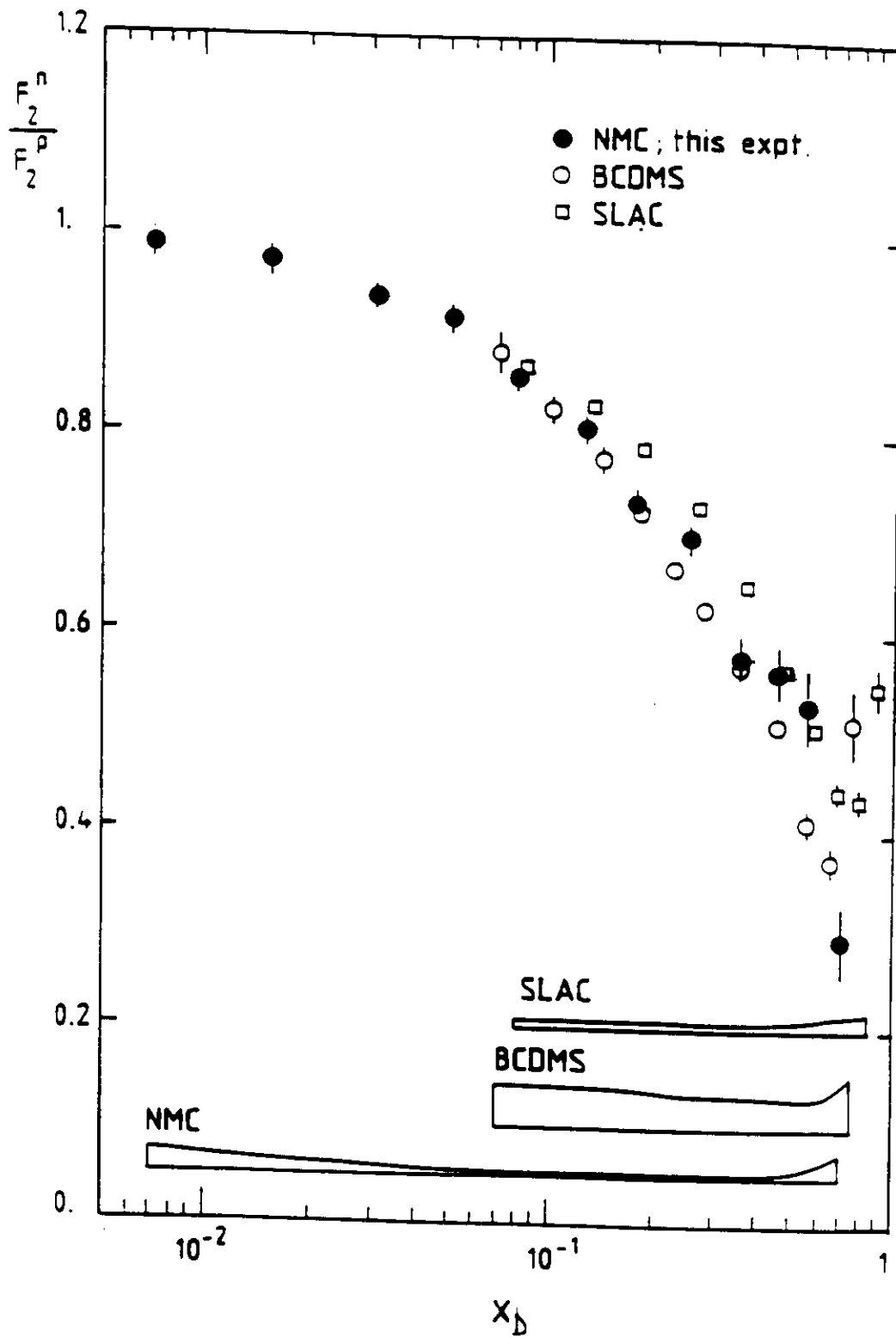
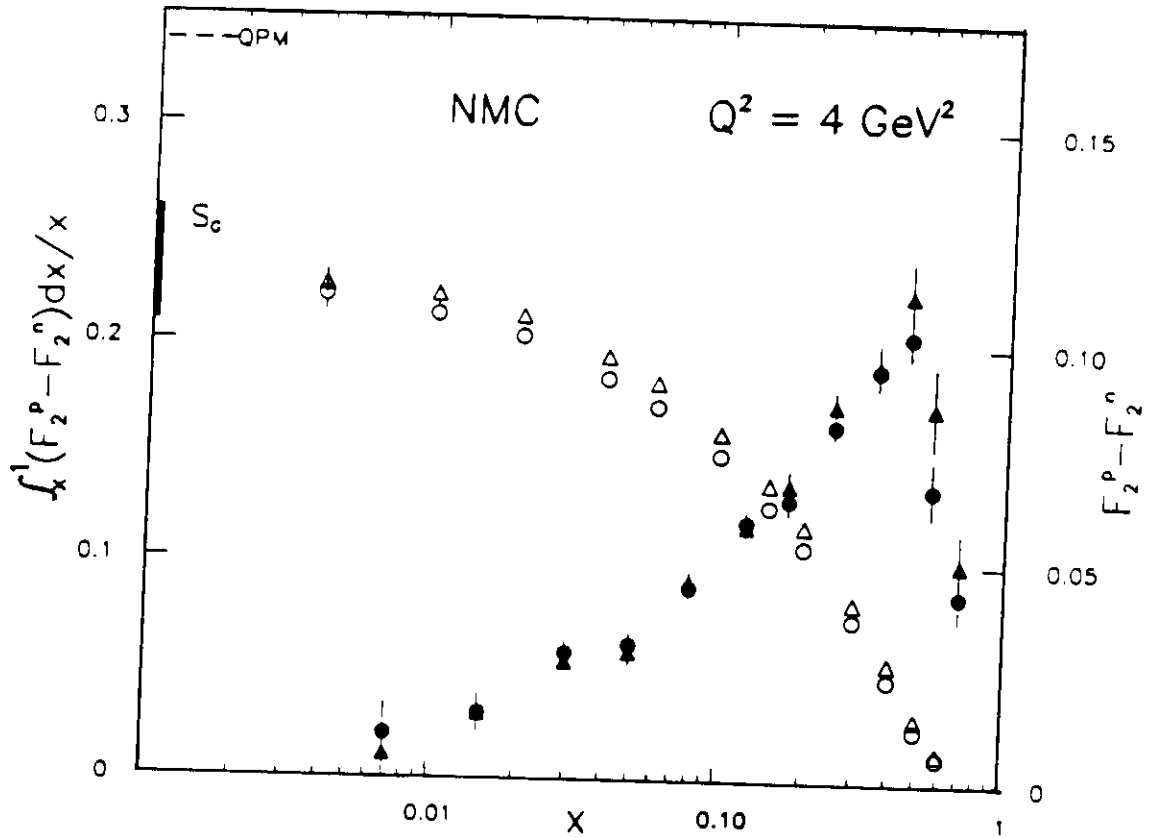
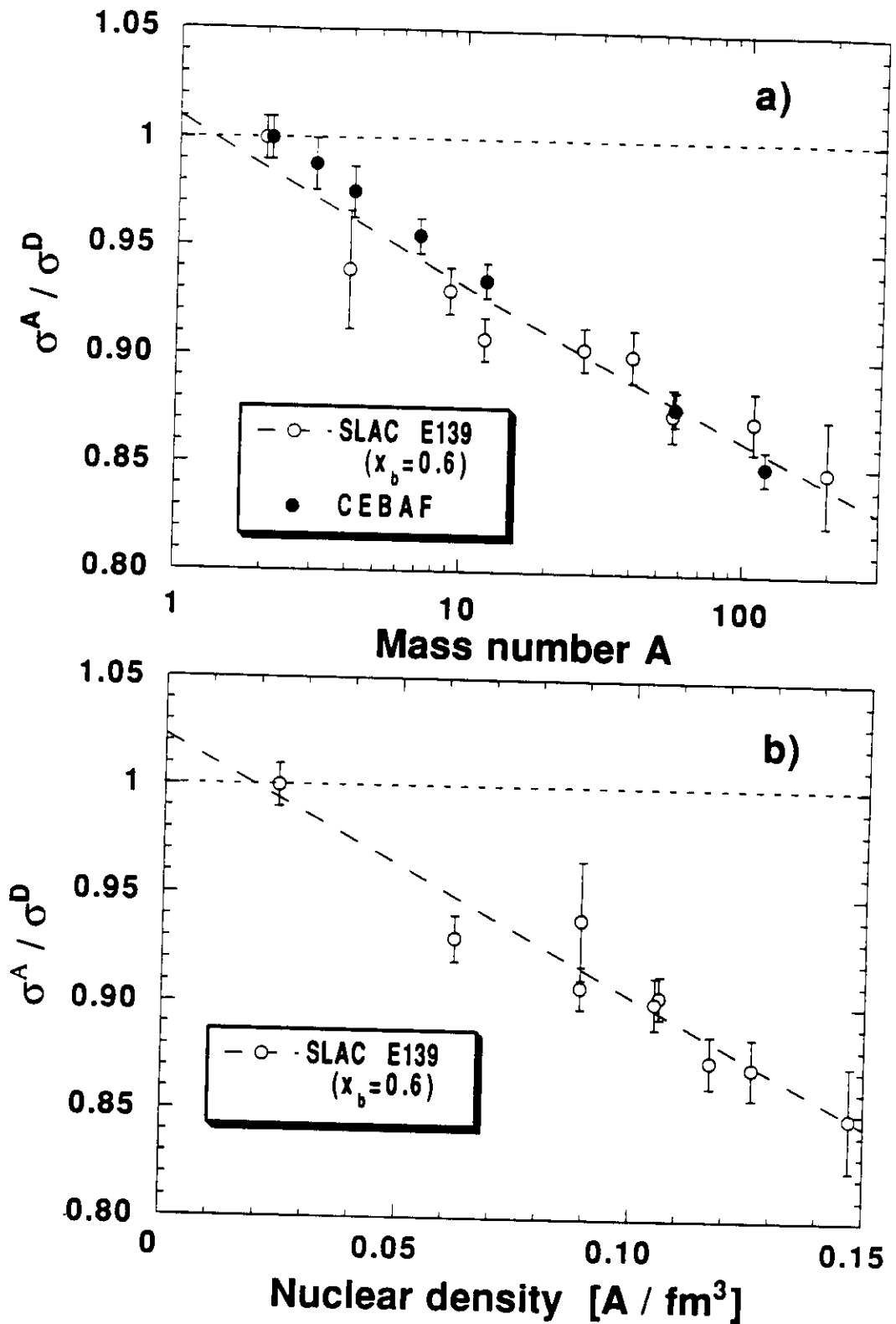


Fig 2.  $F_2^n / F_2^p$  as function of  $x_b$  (from ref.<sup>[11]</sup>).



**Fig 3.** The difference  $F_2^p - F_2^n$  and the Gottfried Sum Rule at  $Q^2 = 4\text{GeV}^2$ . (data from ref.<sup>[13]</sup>). The extrapolated result  $S_G$  is indicated by the bar. The simple quark-parton model (QPM) prediction is also shown.



**Fig 4a.** Ratios  $(\sigma^A / \sigma^D)^{[6]}$  versus atomic weight  $A$  at  $x_b = 0.6$ . Solid line is a model fit of the data as a power law of  $A$ . Also shown are the CEBAF projected data with total errors (statistical+total systematic).

**Fig 4b.** Ratios  $(\sigma^A / \sigma^D)^{[6]}$  versus nuclear density at  $x_b = 0.6$ . Solid line is a model fit of the data as a linear dependence of nuclear density.

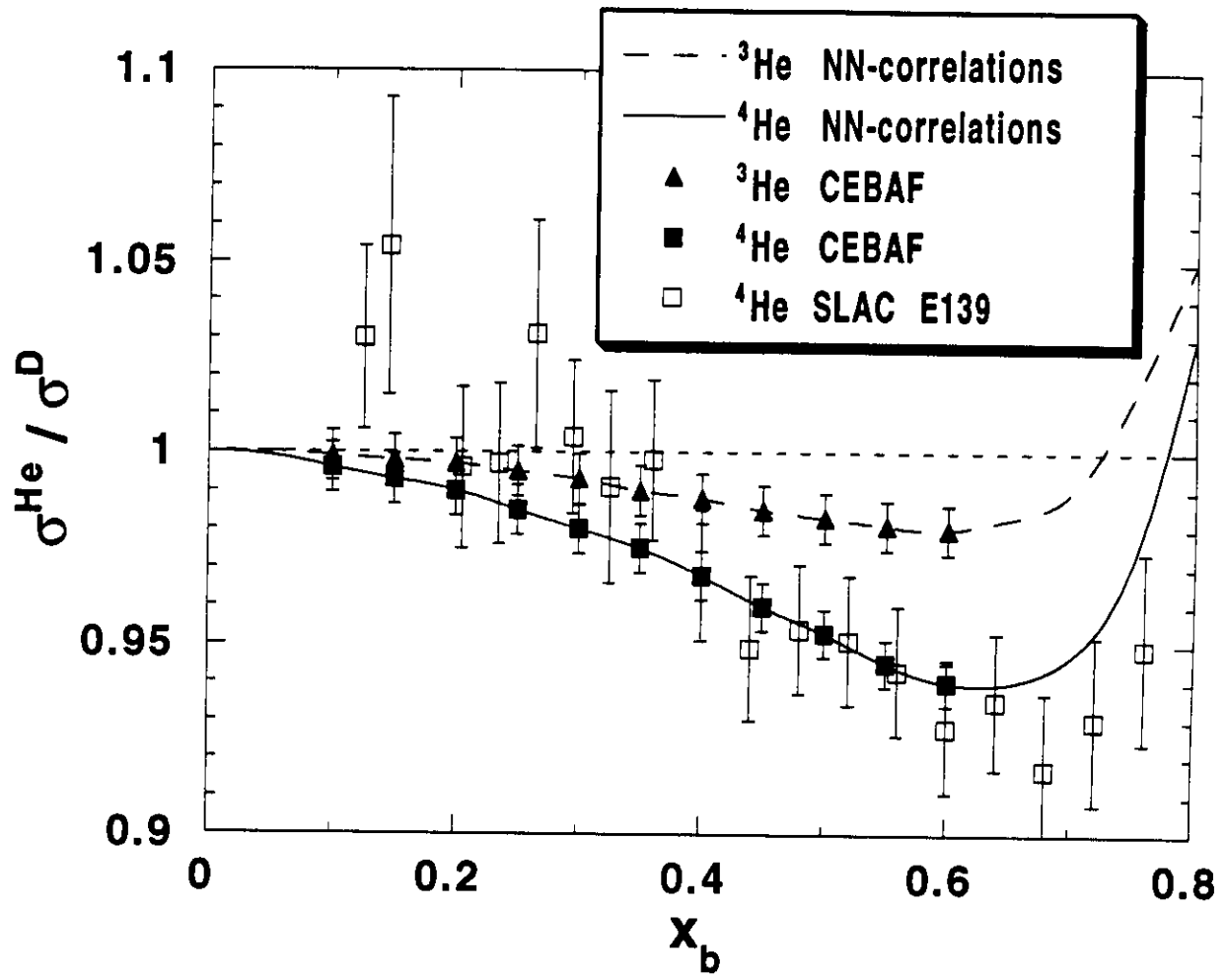


**Fig 5.**  $^3\text{He}$  and  $^4\text{He}$  predictions from pure nucleonic theory (from ref. [12]). Also shown are the  $^4\text{He}$  SLAC E139 previous data and the CEBAF  $^3\text{He}$  and  $^4\text{He}$  projected data with total errors (statistical and point to point systematic).

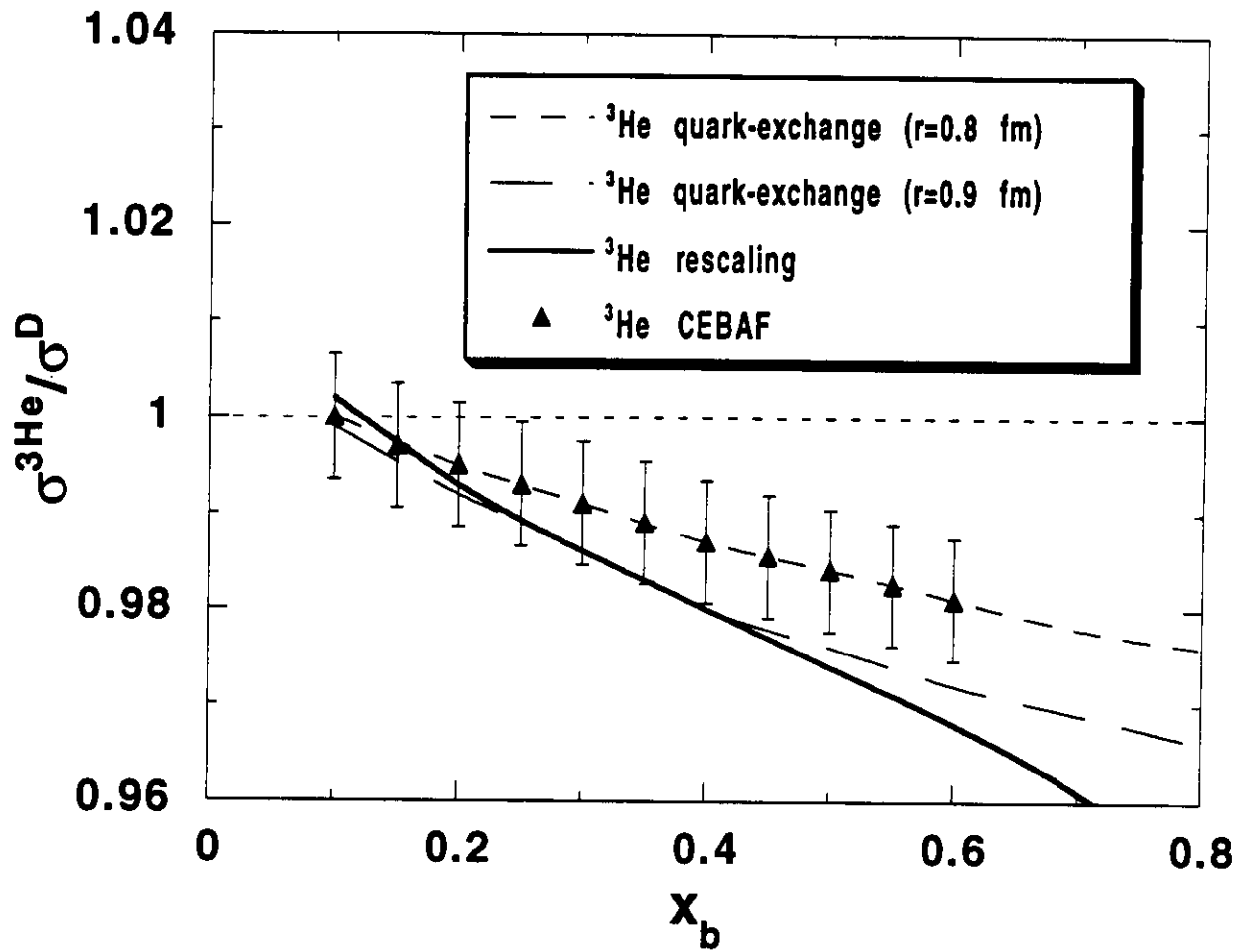


**Fig 6.**  $^3\text{He}$  prediction from the quark-exchange model for two nucleon radii ( $r$ ) and from a rescaling model (from ref. [20]). Also shown are the CEBAF  $^3\text{He}$  and projected data with total errors (statistical and point to point systematic).

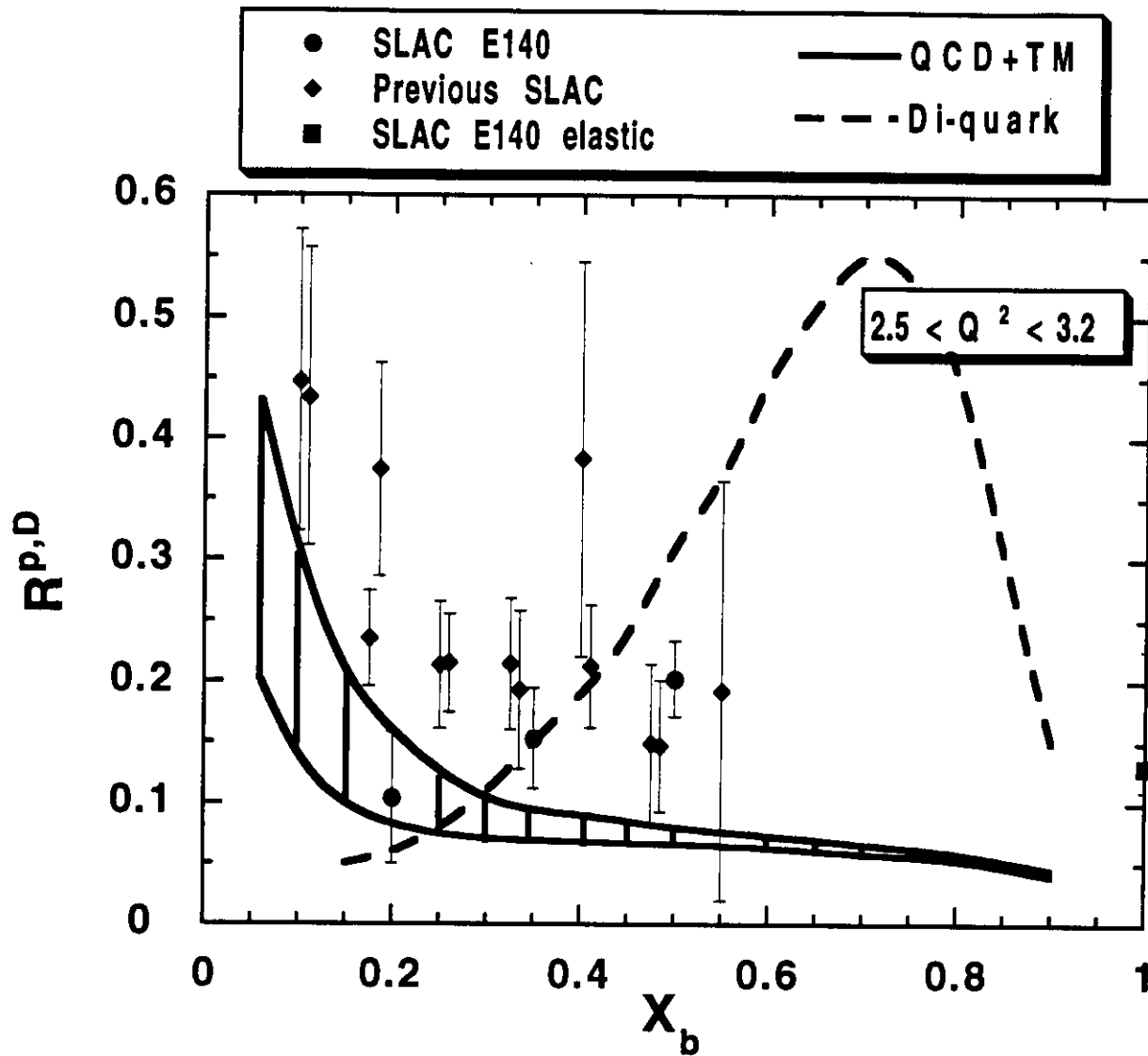
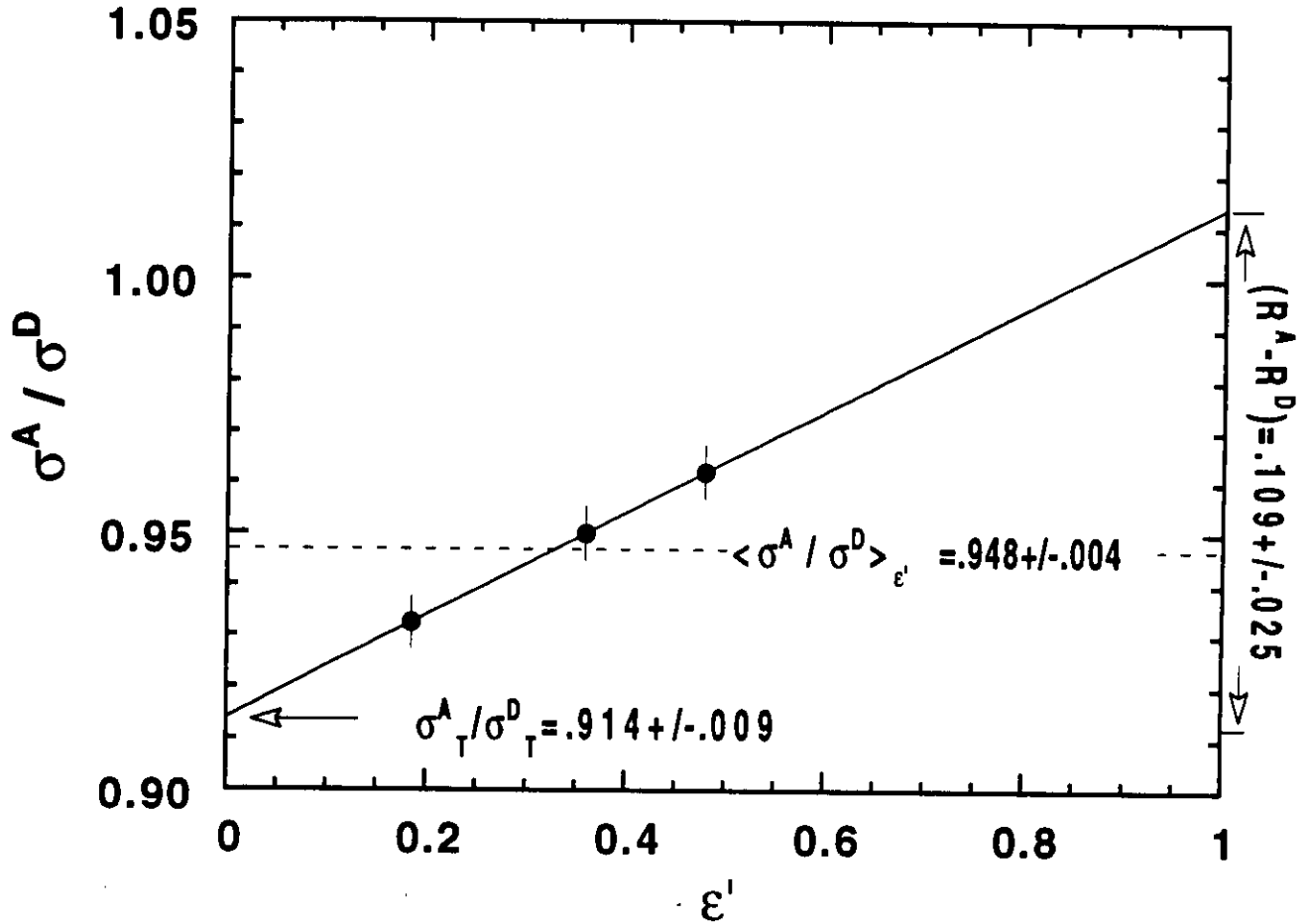
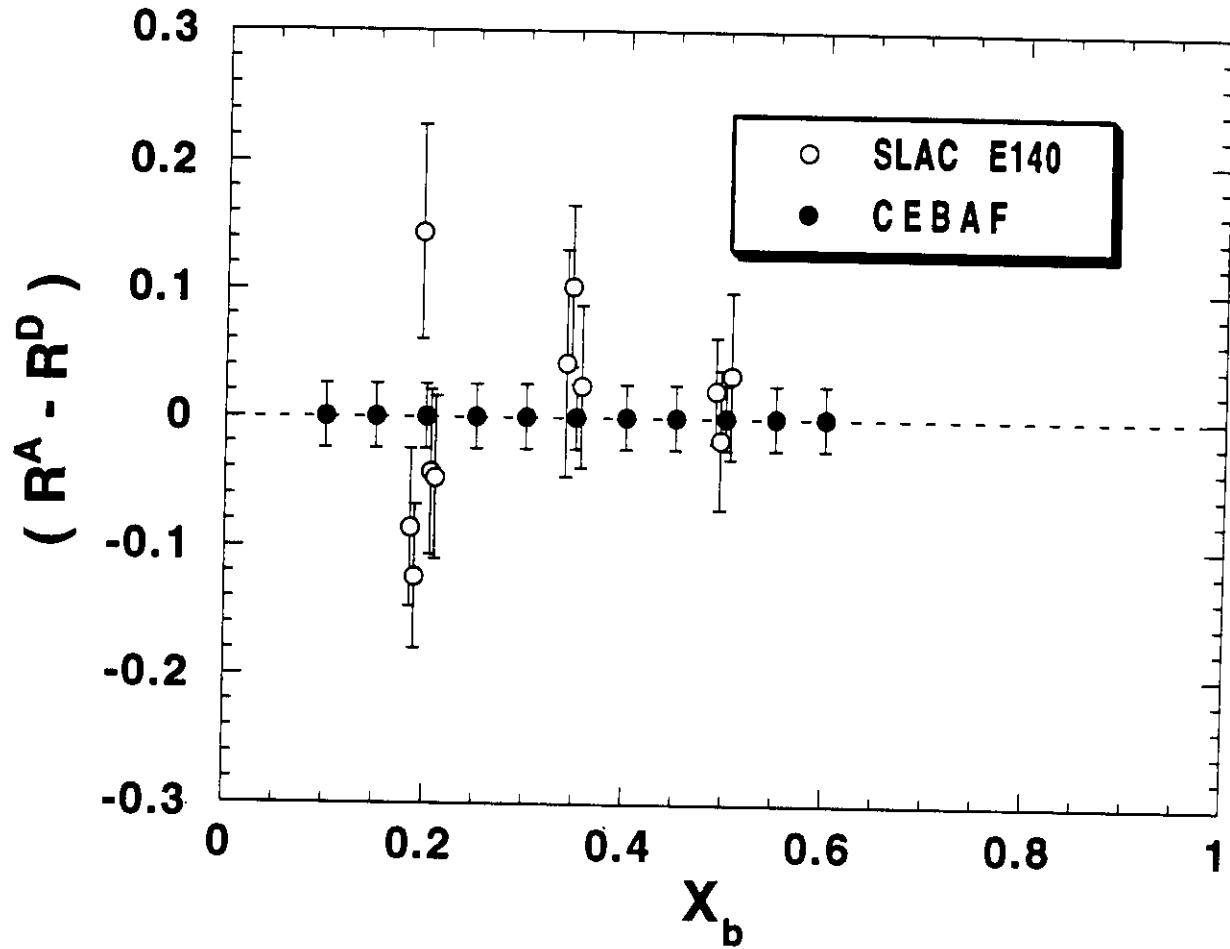


Fig 7. Structure Function  $R(x_b)$  as function of  $x_b$  for intermediate values of  $Q^2$  [7]. The dashed area is the range of QCD calculations including target mass effects, while dashed curve is the prediction of a diquark model neglecting all other contributions<sup>[22]</sup>.

$$\sigma^A / \sigma^D = \sigma^A_T / \sigma^D_T [1 + \varepsilon' (R^A - R^D)]$$



**Fig 8.** Typical expected determination of the quantity  $(R^A - R^D)$  for the CEBAF proposed experiment, with reasonable numbers and total errors.



**Fig 9.**  $(R^A - R^D)$  versus  $x_b$  measured by SLAC E140<sup>[7]</sup> compared with our projected data. Error bars are total error (statistical + point to point systematic).

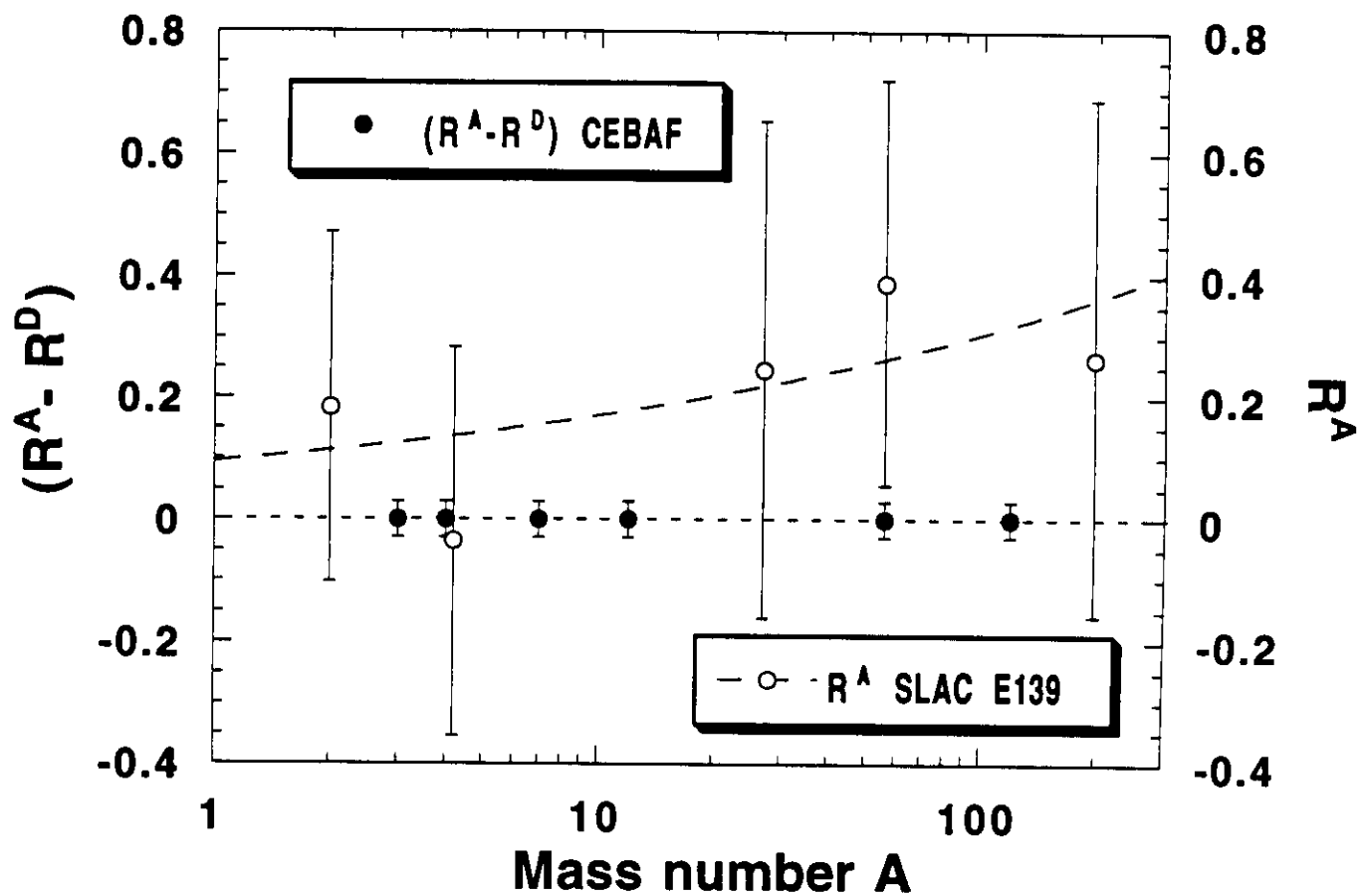
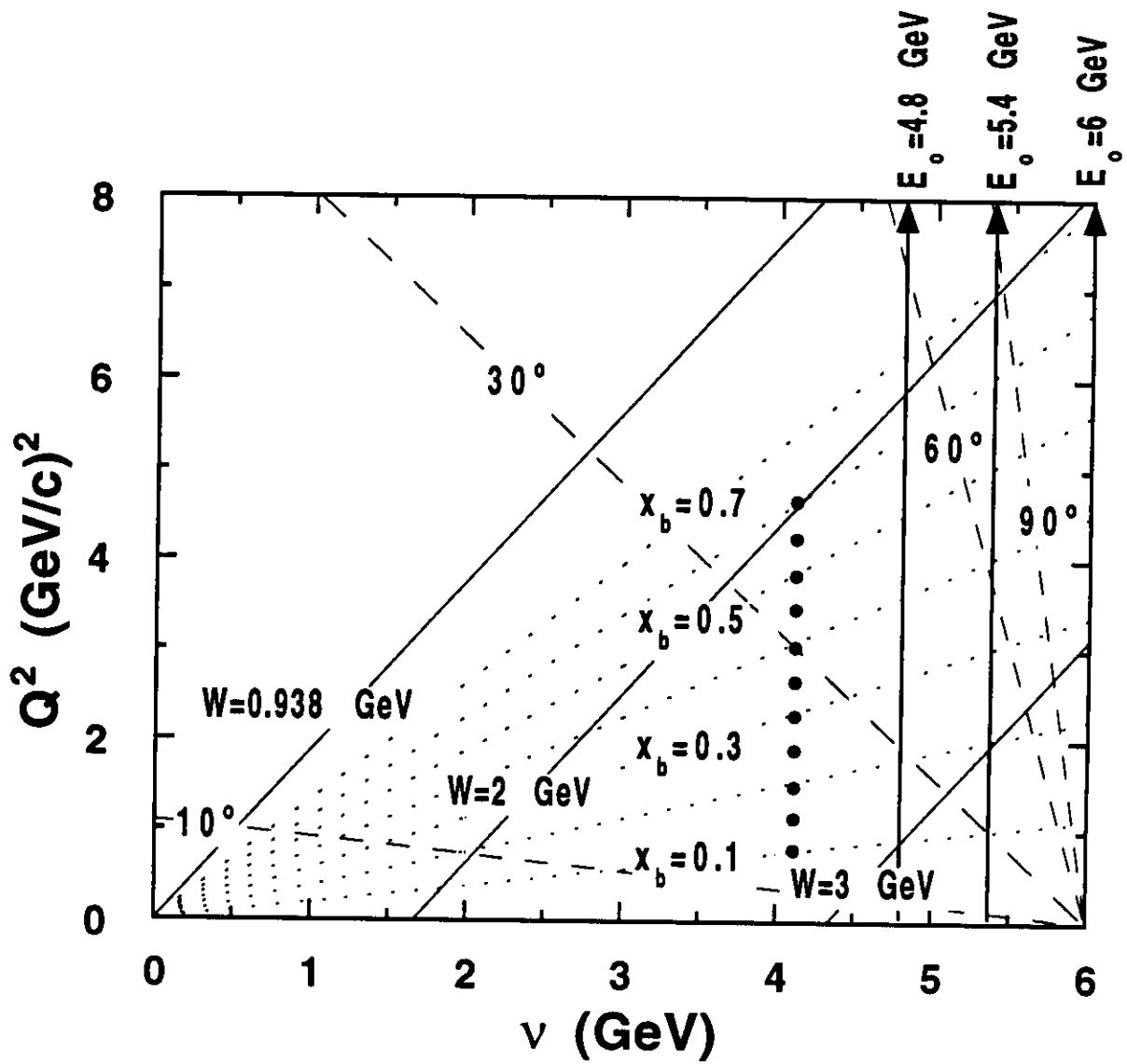


Fig 10.  $R^A$  versus atomic weight  $A$  measured by SLAC E139<sup>[5]</sup> compared with our projected data for  $(R^A - R^D)$ . Error bars are total error (statistical + total systematic).



**Fig 11.** Kinematic plane for inclusive electron scattering ( $e,e'$ ) with a 6 GeV maximum beam energy. Close circles indicate the kinematic points for this proposal for measuring  $\sigma$ ,  $F_2$  and  $R$ .

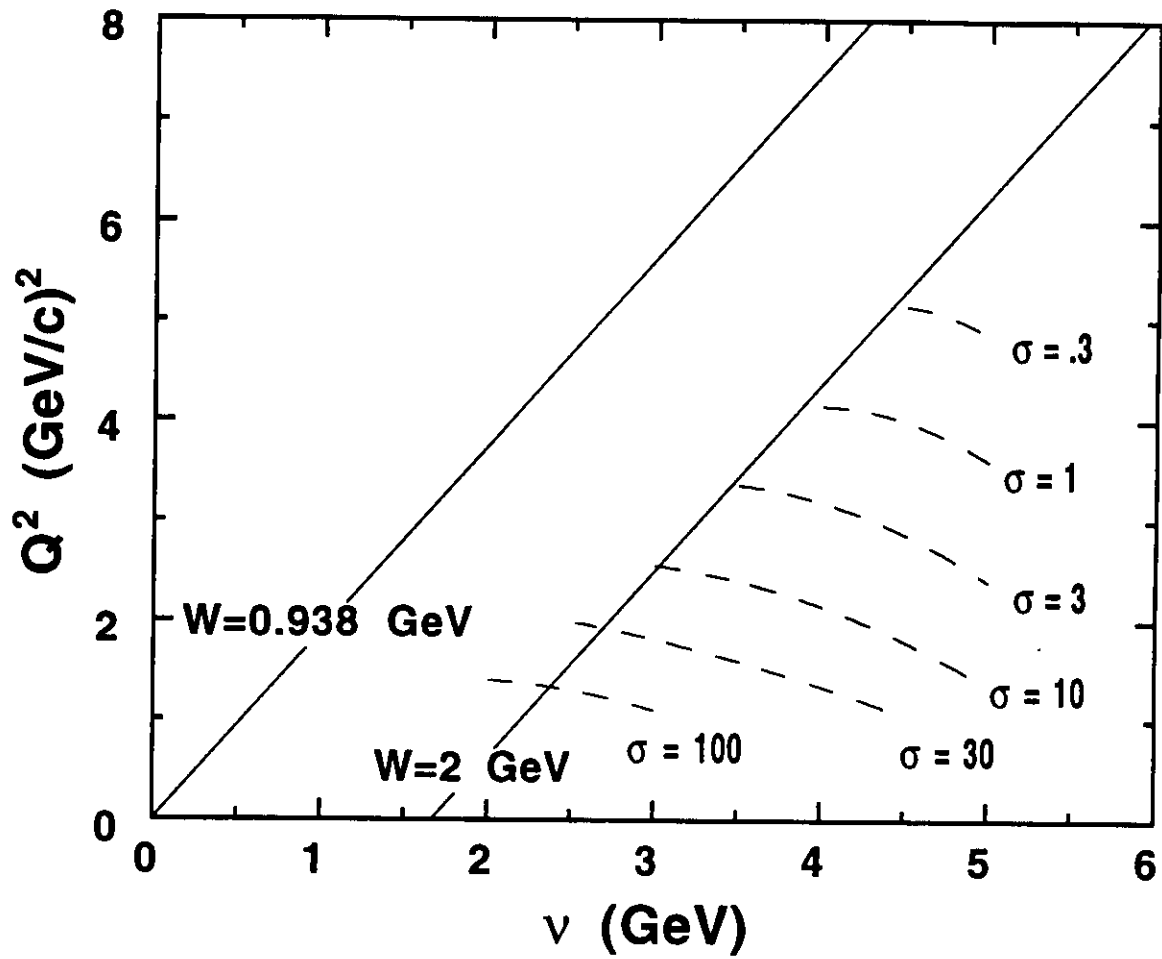


Fig 12. Curves for constant cross section (in  $\text{nb GeV}^{-1} \text{ sr}^{-1}$ ) at 6 GeV.

# LAB RESOURCES REQUIREMENTS LIST

CEBAF Proposal No.: PR 94-100  
(For CEBAF User Liaison Office use only.)

Date: Dec 13, 1994

List below significant resources — both equipment and human — that you are requesting from CEBAF in support of mounting and executing the proposed experiment. Do not include items that will be routinely supplied to all running experiments, such as the base equipment for the hall and technical support for routine operation, installation, and maintenance.

**Major Installations** (either your equip. or new equip. requested from CEBAF)

None

---

---

---

---

---

---

---

---

---

---

New Support Structures: None

---

---

---

**Major Equipment**

Magnets	<u>Standard Base Equipment</u>
Power Supplies	<u>"</u>
Targets	<u>Cryo Targets (<math>\leq 400</math> Watts) Solid Targets (<math>^7\text{Li}</math>, <math>^{12}\text{C}</math>, <math>^{58}\text{Fe}</math>, <math>^{118}\text{S}</math>)</u>
Detectors	<u>"</u>
Electronics	<u>"</u>
Computer Hardware	<u>"</u>
Other	<u>"</u>

**Data Acquisition/Reduction**

Computing Resources: Standard Base Equipment

---

---

---

New Software: \_\_\_\_\_

---

---

---

**Other**

---

---

---

---

---

# HAZARD IDENTIFICATION CHECKLIST

CEBAF Proposal No.: PR 94 - 100  
(For CEBAF User Liaison Office use only.)

Date: Dec 13, 1994

Check all items for which there is an anticipated need.

<p><b>Cryogenics</b></p> <p><input type="checkbox"/> beamline magnets</p> <p><input type="checkbox"/> analysis magnets</p> <p><input checked="" type="checkbox"/> target</p> <p>* { type: <u>LH<sub>2</sub>, LD<sub>2</sub>, <sup>3,4</sup>He(gas)</u></p> <p style="margin-left: 20px;">flow rate: <u>&gt;10 m/s</u></p> <p style="margin-left: 20px;">capacity: <u>20000 litres (STP)</u></p>	<p><b>Electrical Equipment</b></p> <p><input type="checkbox"/> cryo/electrical devices</p> <p><input type="checkbox"/> capacitor banks</p> <p><input type="checkbox"/> high voltage</p> <p><input type="checkbox"/> exposed equipment</p>	<p><b>Radioactive/Hazardous Materials</b></p> <p>List any radioactive or hazardous/toxic materials planned for use:</p> <p>_____</p> <p>_____</p> <p>_____</p>
<p><b>Pressure Vessels</b></p> <p><input type="checkbox"/> inside diameter</p> <p><input type="checkbox"/> operating pressure</p> <p><input type="checkbox"/> window material</p> <p><input type="checkbox"/> window thickness</p>	<p><b>Flammable Gas or Liquids</b></p> <p>* { type: <u>LH<sub>2</sub>, LD<sub>2</sub></u></p> <p style="margin-left: 20px;">flow rate: <u>&gt;10 m/s</u></p> <p style="margin-left: 20px;">capacity: <u>20000 litres (STP)</u></p> <p><b>Drift Chambers</b></p> <p>type: _____</p> <p>flow rate: _____</p> <p>capacity: _____</p>	<p><b>Other Target Materials</b></p> <p><input type="checkbox"/> Beryllium (Be)</p> <p><input checked="" type="checkbox"/> Lithium (Li)</p> <p><input type="checkbox"/> Mercury (Hg)</p> <p><input type="checkbox"/> Lead (Pb)</p> <p><input type="checkbox"/> Tungsten (W)</p> <p><input type="checkbox"/> Uranium (U)</p> <p><input type="checkbox"/> Other (list below)</p> <p>_____</p> <p>_____</p>
<p><b>Vacuum Vessels</b></p> <p><input type="checkbox"/> inside diameter</p> <p><input type="checkbox"/> operating pressure</p> <p><input type="checkbox"/> window material</p> <p><input type="checkbox"/> window thickness</p>	<p><b>Radioactive Sources</b></p> <p><input type="checkbox"/> permanent installation</p> <p><input type="checkbox"/> temporary use</p> <p>type: _____</p> <p>strength: _____</p>	<p><b>Large Mech. Structure/System</b></p> <p><input type="checkbox"/> lifting devices</p> <p><input type="checkbox"/> motion controllers</p> <p><input type="checkbox"/> scaffolding or</p> <p><input type="checkbox"/> elevated platforms</p>
<p><b>Lasers</b></p> <p>type: _____</p> <p>wattage: _____</p> <p>class: _____</p> <p>Installation:</p> <p style="margin-left: 20px;"><input type="checkbox"/> permanent</p> <p style="margin-left: 20px;"><input type="checkbox"/> temporary</p> <p>Use:</p> <p style="margin-left: 20px;"><input type="checkbox"/> calibration</p> <p style="margin-left: 20px;"><input type="checkbox"/> alignment</p>	<p><b>Hazardous Materials</b></p> <p><input type="checkbox"/> cyanide plating materials</p> <p><input type="checkbox"/> scintillation oil (from)</p> <p><input type="checkbox"/> PCBs</p> <p><input type="checkbox"/> methane</p> <p><input type="checkbox"/> TMAE</p> <p><input type="checkbox"/> TEA</p> <p><input type="checkbox"/> photographic developers</p> <p><input type="checkbox"/> other (list below)</p> <p>_____</p> <p>_____</p>	<p><b>General:</b></p> <p>Experiment Class:</p> <p><input checked="" type="checkbox"/> Base Equipment</p> <p><input type="checkbox"/> Temp. Mod. to Base Equip.</p> <p><input type="checkbox"/> Permanent Mod. to Base Equipment</p> <p><input type="checkbox"/> Major New Apparatus</p> <p>Other: _____</p> <p>_____</p>
<p>* From CEBAF CDR (1990) for 1000 Watt Cryo Target Design                  This Experiment requires ONLY 300 - 400 Watts.</p>		

# BEAM REQUIREMENTS LIST

CEBAF Proposal No.: PR94-100

Date: Dec 13, 1994

(For CEBAF User Liaison Office use only.)

List all combinations of anticipated targets and beam conditions required to execute the experiment. (This list will form the primary basis for the Radiation Safety Assessment Document (RSAD) calculations that must be performed for each experiment.)

Condition #	Beam Energy (MeV)	Beam Current (μA)	Polarization and Other Special Requirements (e.g., time structure)	Target Material (use multiple rows for complex targets — e.g., w/windows)	Target Material Thickness (mg/cm <sup>2</sup> )		
1	6000	60		LH <sub>2</sub>	1065		
				LD <sub>2</sub>	2350	}	
				<sup>3</sup> He (gas)	2500		(≈ 350 mths)
				<sup>4</sup> He (gas)	2500		
2	6000	60		<sup>7</sup> Li	3310		
				<sup>12</sup> C	1700	}	
				<sup>58</sup> Fe	550		4% X <sub>0</sub>
				<sup>118</sup> Sn	350		
3	5400	60					
				"	Same set		
					of Targets		
				v	as 1 & 2		
4	4800	60					
				"	Same set		
					of Targets		
				v	as 1 & 2		

Beam energies,  $E_{\text{Beam}}$ , available are:  $E_{\text{Beam}} = N \times E_{\text{Linac}}$  where  $N = 1, 2, 3, 4, \text{ or } 5$ . For 1995,  $E_{\text{Linac}} = 800$  MeV, i.e., available  $E_{\text{Beam}}$  are 800, 1600, 2400, 3200, and 4000 MeV. Starting in 1996, in an evolutionary way (and not necessarily in the order given) the following additional values of  $E_{\text{Linac}}$  will become available:  $E_{\text{Linac}} = 400, 500, 600, 700, 900, 1000, 1100, \text{ and } 1200$  MeV. The sequence and timing of the available resultant energies,  $E_{\text{Beam}}$ , will be determined by physics priorities and technical capabilities.